J-Researchers

JOURNAL OF CIVIL ENGINEERING RESEARCHERS

Evaluation of an aftershock Effect on Steel moment frame structures in various soil types

Javad Pourali[a] , Ehsan Omranian[b] , Gholamreza Abdollahzadeh[b],*

[a] Engineering Faculty, Chaloos Branch, Islamic Azad University, Chaloos 46615-397, Iran

[b] Faculty of Civil Engineering, Babol Noshirvani University of Technology, Babol, Iran

Article History: Received 30 December 2021; accepted 19 February 2022.

Abstract

The aftershocks may weaken or collapse structures that were previously damaged under the main earthquake and have not yet been repaired. In this paper, the seismic performance of an 8-story Steel moment frame structures designed in four types of soil is evaluated under the seismic sequence of earthquake and aftershock. The results showed that the seismic performance of the studied frame under the influence of severe aftershocks can be significantly different from the main earthquake mode alone. For example, in type 1 soil, aftershocks can increase the structure displacement by more than 50% compared to the main earthquake mode alone. It was also found that most aftershocks cause a significant increase in the durable displacement of the roof and in a small number of cases it also reduces it. In addition, the impact of aftershocks on the building damaged by the main earthquake will be much greater than in the case in which the structure under the main earthquake has not suffered much damage.

"Keywords: Aftershock, Mainshock, Seismic sequence, Steel moment frame, Residual inter-story drifts"

1. Introduction

The earthquake is a natural phenomenon that has repeatedly horrled man in human history and has destroyed many cities and villages along with severe human and financial casualties. Historical evidence has shown that large earthquakes are often followed by repeated aftershocks and form a sequence of earthquakes and aftershocks. Strong aftershocks can increase the level of damage to structures with new damage and may also cause weakening or collapse of structures that were previously damaged under the main earthquake. (But, due to the short time between the occurrence of the aftershock and the main earthquake, they have not been repaired yet)[1]. An example of this is the main earthquake in Chile on February 27, 2010 (Mw = 8.8), which caused severe damage to the southern and central regions of Chile with 360 aftershocks with a magnitude of more than5 between February 27 and April 26. Among these aftershocks were 21 magnitudes greater than 6 [9]. The first analytical study on the nonlinear behavior of single-degree-of-liberty (SDOF) systems exposed to the time-history records of the 1972 Managua Post-

Earthquake was conducted by Mahin (1980). He observed that displacement demand ductility (the ratio of maximum inelastic displacement to system yield displacement) in elastoplastic SDOF systems at the end of the main aftershock increases slightly relative to the original earthquake. Mahin examined the effects of this sequence on structures by setting two records of major earthquake and aftershock. This had one major drawback; it did not take into account the effects of the system's free vibration on the distance between the main earthquake and the aftershock. In subsequent studies, a time interval between the main earthquake and the aftershock was considered and it was assumed that at this distance the system would stop moving. Later, some other researchers used a distance of 20 to 100 seconds in their research depending on the type of structures [4,5]. In fact, this time interval is considered only to end the free vibration time of the system, which by examining the behavior of the structures studied in this study, 40 seconds was found to be a suitable number. Figure 1 shows a schematic of how earthquake and aftershock acceleration maps are placed one after the other.

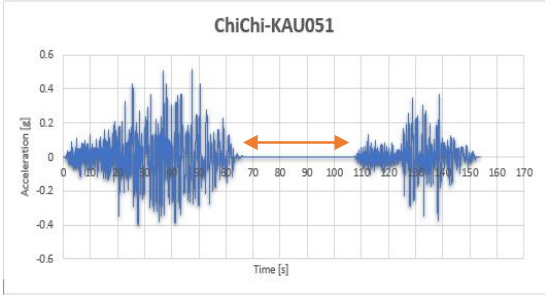

figure 1. How to place the acceleration of earthquake and aftershock

Garcia (2012) examined the characteristics of a wide range of earthquakes and corresponding aftershocks on the seismic response of buildings and showed that the dominant period, as well as the duration of the main earthquake and aftershocks, were statistically weakly correlated. Therefore, the production of artificial seismic sequences from the main earthquake as a basis for the production of aftershocks, even with a smaller amplitude, does not make sense because the frequency and duration of the earthquake are completely different [7]. Therefore, it can be said that it is necessary to use real data to evaluate the performance of existing structures under seismic sequences. Abdullahzadeh et al. (2017) with the help of real seismic sequences and by examining the energy distribution in buildings designed by conventional elastic methods as well as modern plastic design methods based on performance, found that aftershocks have a destructive effect on floors that suffer more damage under the main earthquake. Have seen will have [8]. Recently, several researches have been conducted in the field of seismic evaluation of structures under seismic sequences, in all of which the effect of aftershock in increasing the vulnerability of the structure has been confirmed [10,11]. However, design codes still do not explicitly consider the effects of aftershocks and the cumulative damage caused by them in the design of earthquake-resistant structures. The reason for this is probably due to the many uncertainties in the capacity of structures damaged after the main earthquake, the complexity of aftershock characteristics and the probability of their occurrence and the general lack of system fragility models to evaluate the performance of structures [2, 12].

2. Modeling

To evaluate the vulnerability of MDOF structures (several degrees of freedom) under the effect of earthquake and aftershock sequence, an 8-story building in Tehran of medium steel bending frame type in 4 types of soil (A, B, C, & D) based on LRFD method Article 10 of the National Building Code and the fourth edition of Standard 2800 [6] were designed. These structures have three openings of 5 meters in each direction and the height of the floors is 3.2 and the height of the parking lot is 2.7. First, the design of this building was done according to the residential use and located on a relatively high-risk area according to the definition of 2800 standard with the help of Etabs software. Then, for two-dimensional analysis of the critical frame, the selection and seismic performance of this frame were evaluated using time history analyzes by applying natural earthquake and aftershock records using OpenSees finite element software. Figure 3 shows the three-dimensional and two-dimensional views of the designed frame.

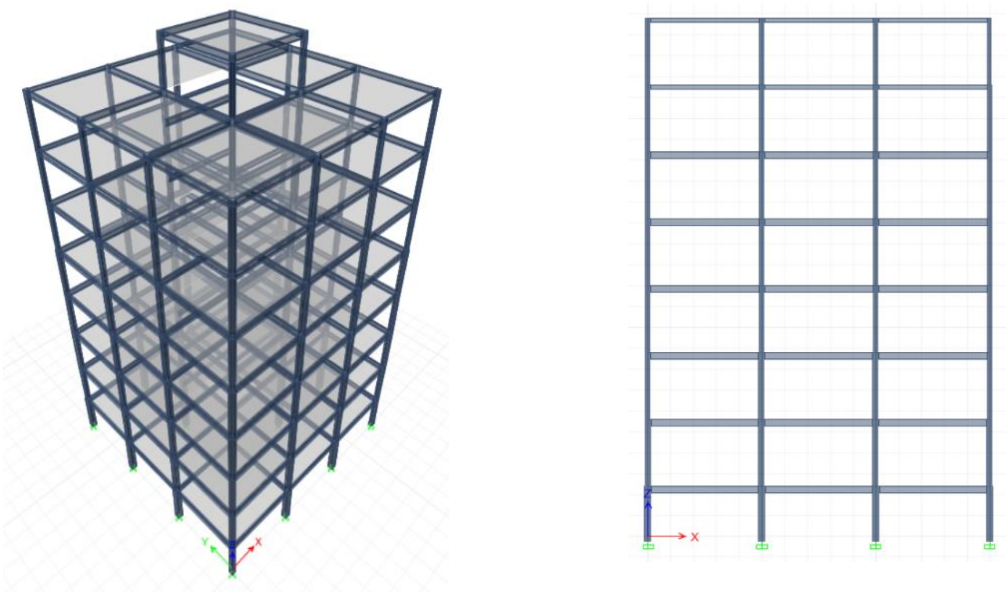

Figure 3. Three-dimensional and two-dimensional view of the designed frame

In the definition of steel, non-linear materials (steel02) in the OpenSees material library were used and the cross-section of the members was made of fiber.This command separates the cross section into smaller areas and summarizes the stress-strain response of the materials for these areas to obtain the resultant behavior. Tables 1 and 2 provide a list of sections designed in the critical frame.

Table No. 1- List of designed beam sections

Type C soil	Type C soil	Type B soil	Type A soil
PG-W180X6-F150X10	PG-W180X6-F150X8	IPE180	**PG-W180X6-F150X8**
PG-W240X6-F150X12	PG-W180X6-F150X15	IPE240	**PG-W180X6-F150X10**
PG-W240X6-F150X15	PG-W300X6-F150X10	IPE270	**PG-W200X8-F150X10**
PG-W350X6-F150X20	PG-W300X6-F150X12	IPE300	**PG-W240X6-F150X8**
PG-W400X6-F150X12	PG-W300X6-F150X15	PG-W250X8-F200X12	**PG-W300X6-F150X10**
PG-W400X6-F150X25	PG-W300X6-F150X20	PG-W250X8-F200X15	**PG-W240X6-F150X12**
		PG-W300X8-F200X15	

Table 2 - List of designed sections of the column

Type C soil	Type C soil	Type B soil	Type A soil
BOX240X15	BOX180X8	BOX150X10	BOX180X8
BOX250X8	BOX200X8	BOX200X10	BOX200X8
BOX250X10	BOX200X10	BOX200X12	BOX200X10
BOX250X12	BOX200X12	BOX200X15	BOX240X10
BOX250X20	BOX240X10	BOX250X10	BOX240X12
BOX300X20	BOX240X12	BOX250X12	BOX240X20
	BOX240X15	BOX250X15	
	BOX240X20	BOX250X20	
	BOX300X20		

Past studies have shown that records must be scaled to the desired hazard level to achieve proper seismic behavior [3]. In this study, 12 raw accelerometers were extracted from PEER site data in accordance with the soil type and were compared and scaled according to the instructions of the fourth edition of the 2800 standard. Table 3 shows the characteristics of each of the corresponding earthquake and aftershock accelerometers.

Table No. 3- Characteristics of earthquake and aftershock acceleration

Soil Type	Name of earthquake	Station	Magnitude of earthquake	magnitude of the aftershock	Shear wave velocity
A	Chi-Chi	HWA002	7.62	6.2	789
	Chi-Chi	KAU051	7.62	6.2	1004
	Northridge	WONDERLAND	6.69	5.28	1222
B	Chi-Chi	CHY074	7.62	6.2	665
	Mamooth	Long valley dam	6.06	5.91	496
	Northridge	Pacoima Kagel Canyon	6.69	5.28	550
C	HOLISTER	Holister	5.6	5.5	198
	Imperial Valley	Holtvile	6.53	5.01	202
	Northwest	Jiashi	6.1	5.8	240
D	Chi-Chi	CHy054	7.62	6.3	172
	Chi-Chi	ILA044	7.62	6.3	160.6
	Whittier	Carson	5.99	5.27	160

It should be noted that regarding the scale of aftershocks, the adaptation coefficient was used to maintain the PGA ratio of earthquake and aftershock. According to Table 4, the ratio of PGA aftershock to the main earthquake is:

TABLE 4 - RATIO OF PGA AFTERSHOCK TO MAIN EARTHQUAKE

SOIL TYPE	Name of earthquake					
A	Chi-Chi-KAU051		Northridge-Wonderland		Chi-Chi-HWA002	
	pga after / pga ma	**-0.7365**	pga after / pga ma	**0.528706**	pga after / pga ma	**0.353661**
B	Chi-Chi-CHY074		Mamooth-Long valley Dam		Northridge-Pacomia	
	pga after / pga ma	**-1.3782**	pga after / pga ma	**1.1206**	pga after / pga ma	**-0.50448**
C	Northwest-Jiashi		Holister-Holister		Imperial-Holtvile	
	pga after / pga ma	**0.873402**	pga after / pga ma	**-0.61133**	pga after / pga ma	**-0.44463**
D	Chi-Chi-CHy054		Whittier-Carson		Chi-CHi-ILA044	
	pga after / pga ma	**-0.80387**	pga after / pga ma	**0.443668**	pga after / pga ma	**0.367758**

3. Comparison of floor drift distribution

The frames are exposed to the seismic sequences of the accelerometers presented in Table 3 under time history analysis, and the drift changes of the classes in height are shown in Figures 1 to 4. As can be seen from the diagrams for floor drift in four soils, aftershocks in some cases lead to a sharp increase in structural drift, for example in the Northridge Earthquake type A soil in some floors (such as the 7 floor). The quake has more than doubled. In the Chi-Chi earthquake, kau041 also increased slightly. But in chici-HWA002 earthquake, no increase in structural drift was observed. This issue is justified by the very low intensity of aftershocks in the recent earthquake. In the chici-HWA002 earthquake, the maximum ground acceleration (PGA) of the aftershock was 35% of the main earthquake and therefore the main damage occurred during the main earthquake And aftershock damage did not have much on the main structure. However, according to the 2800 standard guidelines, if these three records are selected for design, maximum results should be used. Therefore, it is observed that aftershocks can have very destructive effects (increasing displacement up to more than double) that ignoring these effects in the design process can have catastrophic consequences during an earthquake. Another issue that seems to be important is the change of drift direction. . For example, in the structure under study under the Northridge earthquake, the fifth-floor drift caused by the main earthquake is equal to - 0.25% while this value has reached + 0.25% during the aftershock. This change in drift direction may cause severe damage to the structure, and it is possible that the structure will not be able to withstand such a deformation during severe earthquakes.

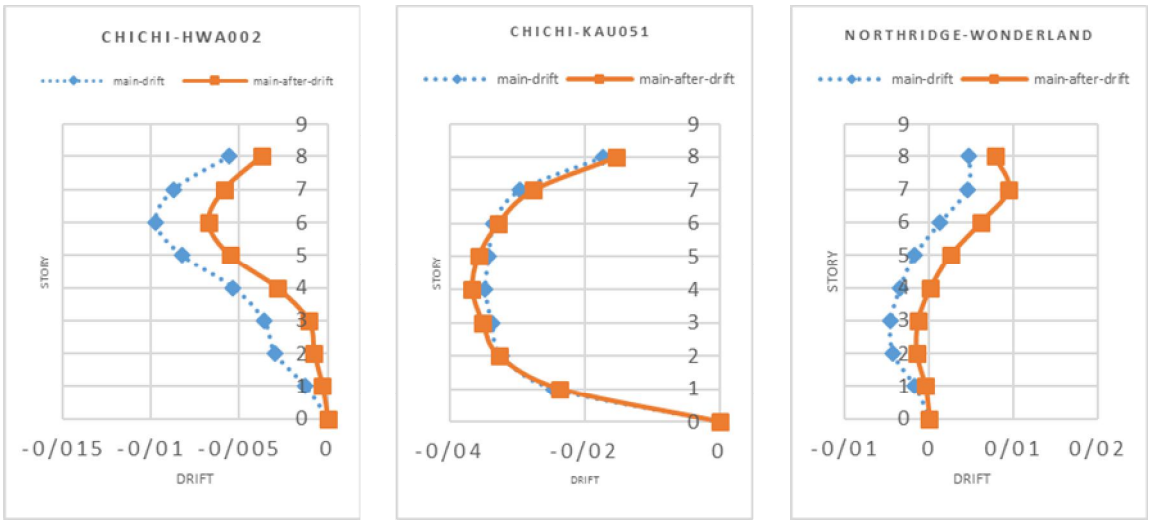

Graphs 1. Type A soil drift change diagrams

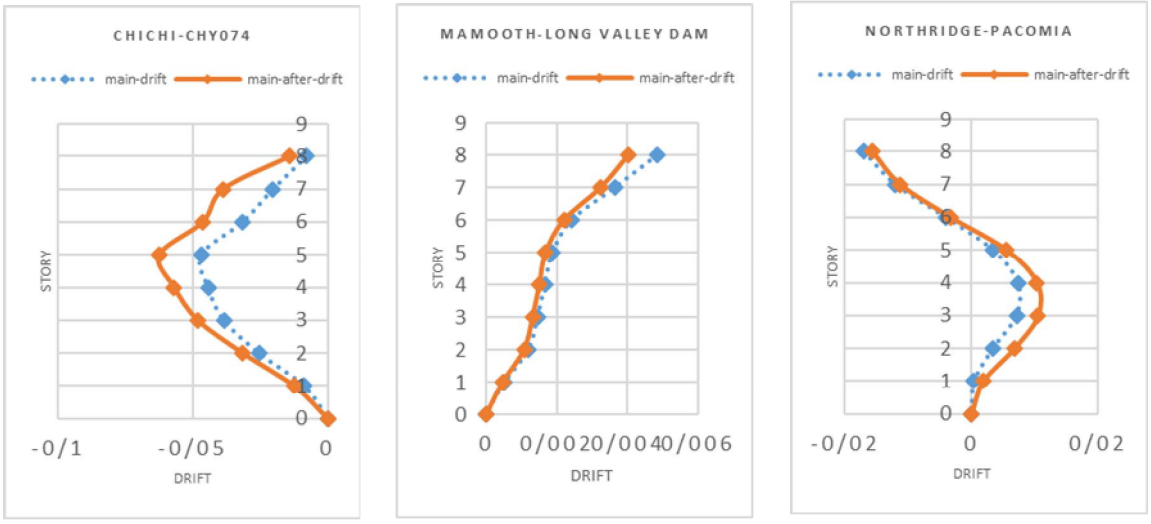

Graphs 2. Type B soil drift change diagrams

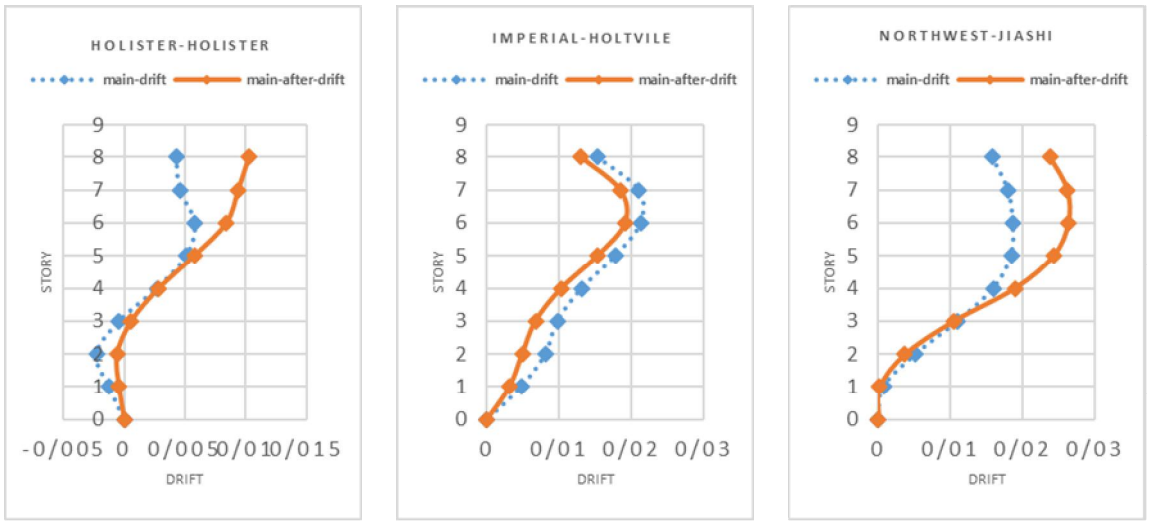

C **B** **A**

Graphs 3. Type C soil drift change diagrams

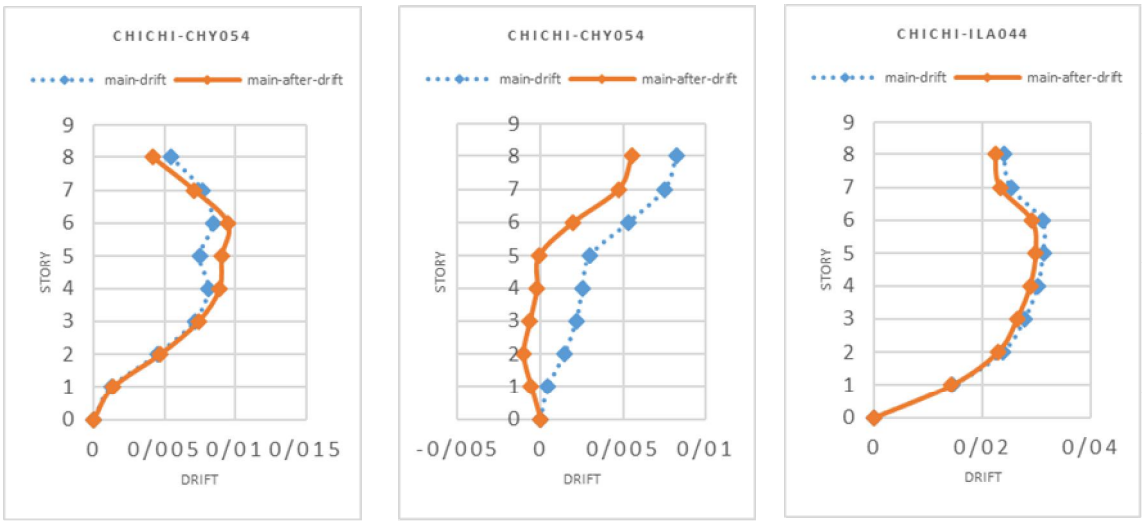

C **B** **A**

Graphs 4. Type D soil drift change diagrams

4. Comparison of permanent displacement distribution of floors

Examining the drift distribution of floors at the collapse level of the damaged structure, it was found that with the increase of damage under the main earthquake, the distribution of damage is more concentrated in the same floors damaged in the main earthquake, while the same record in a healthy structure causes the failure of another floor.Comparison of permanent displacement distribution of floors. Finally, the remaining displacement of the elements in both healthy and damaged structures is investigated. The parameter of relative displacement, which is considered as a good representative for damage to structural members, also strongly depends on the type of damage caused by the main earthquake. The drift changes of the floors in the primary and damaged structures in different soil types are shown in Figures 5 to 9. As can be seen from Figures 5 to 9, the permanent displacement of the roof under the effect of seismic sequence is sometimes less than the permanent displacement of the roof under the effect of the main earthquake alone. This phenomenon expresses the important issue that aftershocks do not necessarily increase the permanent displacement of the structure. In examining the permanent displacement of the roof, it should be noted that the structure may not stop at its maximum permanent displacement due to successive earthquakes and as a result have less permanent displacement, although in this case, the damage to the structure has increased.

Tables 4 to 8 show the ratio of residual displacement of the structure under a series of earthquakes compared to the main earthquake.

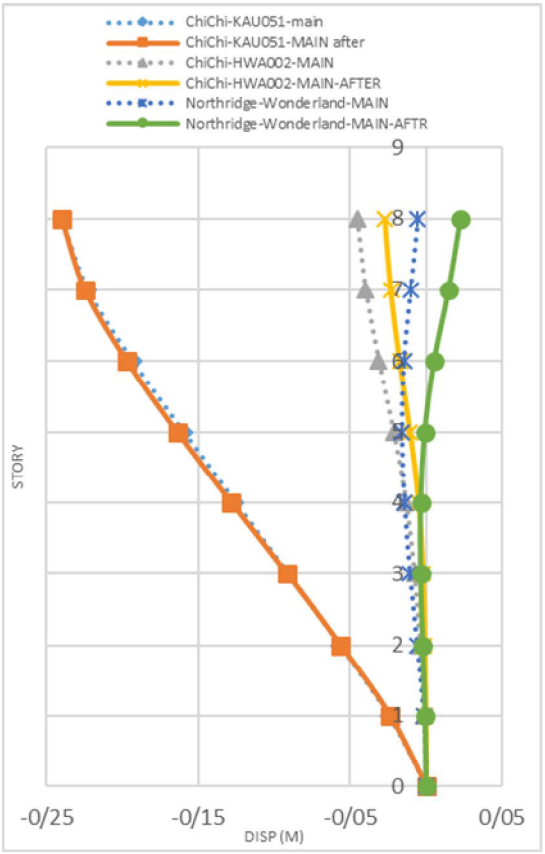

Chart 5. Permanent displacement diagrams Soil type A.

Table 4- Ratio of displacement ratio of the structure under the effect of the seismic sequence in comparison with the main earthquake In type A soil

Record name	floors							
	ST8	ST7	ST6	ST5	ST4	ST3	ST2	ST1
ChiChi-HWA002	0.59	0.58	0.55	0.49	0.38	0.27	0.25	0.24
Northridge-Wonderland	-4.04	-1.42	-0.35	0.06	0.24	0.33	0.34	0.3
ChiChi-KAU051	1	1.01	1.02	1.03	1.02	1.01	0.99	0.96

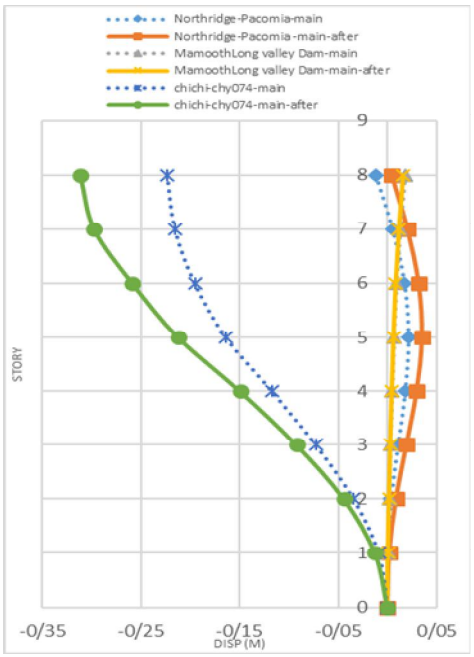

Chart 6. Permanent displacement diagrams Soil type B.

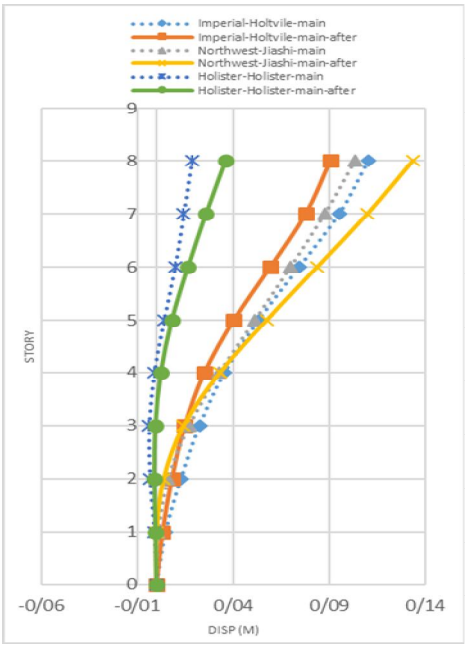

Chart 7. Permanent displacement diagrams Soil type C.

Table 5- Ratio of displacement ratio of the structure under the effect of the seismic sequence in comparison with the main earthquake In type B soil

Record name	floors							
	ST8	ST7	ST6	ST5	ST4	ST3	ST2	ST1
MamoothLong valley Dam	0.88	0.90	0.90	0.90	0.90	0.90	0.90	0.91
NorthridgePacomia	-0.39	3.92	1.82	1.62	1.62	1.77	2.32	4.91
chichichy074	1.40	1.38	1.33	1.30	1.28	1.27	1.29	1.43

Table 6- Ratio of displacement ratio of the structure under the effect of the seismic sequence in comparison with the main earthquake In type C soil

Record name	floors							
	ST8	ST7	ST6	ST5	ST4	ST3	ST2	ST1
MamoothLong valley Dam	0.88	0.90	0.90	0.90	0.90	0.90	0.90	0.91
NorthridgePacomia	-0.39	3.92	1.82	1.62	1.62	1.77	2.32	4.91
chichichy074	1.40	1.38	1.33	1.30	1.28	1.27	1.29	1.43

Table 7- Ratio of displacement ratio of the structure under the effect of the seismic sequence in comparison with the main earthquake In type D soil

Record name	floors							
	ST8	ST7	ST6	ST5	ST4	ST3	ST2	ST1
Imperial-Holtvile	0.82	0.82	0.80	0.76	0.71	0.66	0.63	0.67
Northwest-Jiashi	1.29	1.25	1.20	1.12	1.01	0.85	0.65	0.19
Holister-Holister	1.94	1.81	1.70	2.09	-1.78	0.13	0.30	0.36

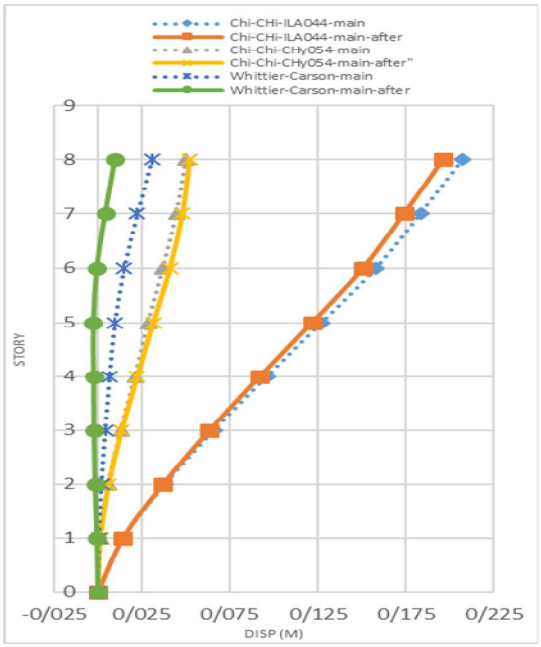

Chart 8. Permanent displacement diagrams Soil type D.

5. Conclusion

To evaluate the response of steel MDOF structures under the effects of seismic sequencing, an 8-story building with medium Steel moment system in 4 types of soil (A, B, C & D) was designed according to version 4 of 2800 standard by LRFD method. Then, the most critical frame of each structure was selected for modeling in opensees software and finally, the performance of steel bending frames was investigated through applying natural records of an original earthquake and scaled aftershock according to standard criteria 2800 in terms of maximum relative displacement within the floor and relatively lasting displacement which is considered as a good representative for structural organ damage and the following results were obtained.

1- The distribution of structural drift in each accelerometer is different. For example, in the acceleration of the Northridge Earthquake type A, the drift of the 6th and 7th floors had the highest increase, but in the 051 earthquake - Chi-Chi, the drift of the 3rd and 4th floors increased. However, aftershocks can sometimes have severe effects on the displacement of the structure and can even increase displacement by more than 50% in the structure (such as soil structure type 1 under earthquake and North Earthquake aftershocks), so aftershocks should be used in conventional designs. Be considered

2- Comparing the residual displacement of the elements in the two healthy and damaged structures, it was found that the residual displacement in the damaged structure is strongly dependent on the type of damage caused in the main earthquake. In fact, depending on the category of damage caused by the earthquake to the healthy structure, the focus of damage in the damaged structure has changed. This result can be seen due to the shape of the behavioral curves for structures with different percentages of damage. In some stimuli, there was no significant difference between the behavior of damaged and healthy structures.

3- By examining the drift distribution of floors in the collapse level of the damaged structure, it was found that with the increase of damage under the main earthquake, the distribution of damage is more concentrated in the same damaged floors in this earthquake, while the same record in a healthy structure causes damage in another floor.

References

1. G. yeo & A. Cornell S(2005)"tochastic Characterization and Decision Bases under Time-Dependent Aftershock Risk in Performance-Based Earthquake Engineering", PEER report.

2. Nazari. N, De Lindt.W, Li.Y,(2015)"Quantifying Changes in Structural Design Needed to Account for Aftershock Hazard", Journal of Structural Engineering.

3. Kiani, J. and Khanmohammadi M. (2015). New approach for selection of real input ground motion records for incremental dynamic analysis

(IDA). Journal of Earthquake Engineering 19, no. 4: 592-623.

4. Mahin SA. (1980) *Effects of duration and aftershocks on inelastic design earthquakes*. In: Proceedings of the seventh world conference on earthquake engineering. vol. 5. p. 677–9.

5. Fragiacomo M, Amadio C, Macorini L. (2004) *Seismic response of steel frames under repeated earthquake ground motions*. Eng Struct;26:2021–35.

6. Earthquake Design Regulations, Standard 7, Edition 4, Building and Housing Research Center, Journal No. Z-1, First Edition 2014

7. Ruiz-Garcia J. Mainshock–aftershock ground motion features and their influence in building's seismic response. Journal of Earthquake Engineering 2012; 16(5):719–37.

8 Abdollahzadeh G.R., Mohammadgholipour A., Omranian E. (2017). Seismic evaluation of steel moment frames under mainshock-aftershock sequence designed by elastic design and PBPD methods Journal of Earthquake Engineering, (accepted).

9. Banon, H.,J.M.Biggs, and H.M.Irvine.."seismic Damage of Reinforced Concrete Frames." Journal of the structural Division,ASCE 107 (ST9) 1713-1981-1729

10. Hosseinpour F., and Abdelnaby A. E. (2017). Fragility curves for RC frames under multiple earthquakes. Soil Dynamics and Earthquake Engineering 98: 222-234.

11. Omranian E, Abdelnaby A. E., Abdollahzadeh Gh.R, Rostamian M., Hosseinpour F., Fragility Curve Development for the Seismic Vulnerability Assessment of Retrofitted RC Bridges under mainshock-aftershock seismic sequences, Structures Congress 2018 (accepted).

12. Abdelnaby, A. E.(2012)"Multiple earthquake effects on degrading reinforced concrete structures." Doctoral dissertation, Univ. of Illinois, Urbana-Champaign, IL.